A Blind Polyphase Time-Domain Selected Mapping for Filtered Single-Carrier Signal Transmission

Amnart Boonkajay* and Fumiyuki Adachi†
*†Research Organization of Electrical Communication (ROEC), Tohoku University
2-1-1 Katahira, Aoba-ku, Sendai, Miyagi, 980-8577 Japan
E-mail: *amnart@riec.tohoku.ac.jp, †adachi@ecei.tohoku.ac.jp

***Abstract*—Single-carrier (SC) signal has a low peak-to-average power ratio (PAPR) property. However, the PAPR of SC signal increases if transmit filtering and/or high-level modulation are applied. We have recently proposed a time-domain selected mapping (TD-SLM) which effectively reduces the PAPR of filtered SC signals by applying the binary phase rotation before transmit filtering, but the necessity of side-information decreases the spectrum efficiency (SE). In this paper, a blind TD-SLM which does not require side-information is proposed. Unlike the frequency-domain SLM (FD-SLM) and the original TD-SLM with side-information, polyphase rotations are used. Performance evaluation of the proposed blind TD-SLM is done by computer simulation assuming turbo-coded filtered SC block signal transmission in aspects of PAPR and bit-error rate (BER) to show that no significant BER performance degradation is occurred.**

***Index Terms*—Single-carrier (SC) transmission, selected mapping (SLM), peak-to-average power ratio (PAPR)**

I. Introduction

Single-carrier (SC) transmission with frequency-domain equalization (FDE) [1] is a robust transmission technique in a frequency-selective fading channel [2]. The SC transmit waveform has a property of low peak-to-average power ratio (PAPR). PAPR of the SC-FDE waveform, however, increases if band-limiting transmit filtering and/or high-level data modulation are applied [3]. High-PAPR signal leads to high power consumption in power amplifier (PA) [4]. Therefore, PAPR reduction of filtered SC-FDE signal remains a significant issue even in the fifth-generation (5G) wireless communication systems which provide broadband data services.

Selected mapping (SLM) [5] is a very attractive signal processing technique since it is a distortionless technique providing effective PAPR reduction. We have recently proposed SLM-based PAPR reduction techniques for SC-FDE, where the phase rotation is applied either in frequency domain or time domain [6-7]. In frequency-domain based SLM (FD-SLM) [6], the phase rotation is applied after discrete Fourier transform (DFT) of data-modulated transmit block and then, frequency-domain transmit filtering and inverse DFT (IDFT) are applied to get a time-domain transmit block. On the other hand, in time-domain based SLM (TD-SLM) [7], the phase rotation is applied directly to data-modulated transmit block before transmit filtering. It was shown in [6-7] that both SLM techniques can effectively reduce the PAPR of filtered SC-FDE. However, the TD-SLM better reduces the PAPR than FD-SLM if the number of phase rotation patterns is the same. Bit-error rate (BER) performance can be kept intact, but the transmission of side-information is required, which degrades the spectrum efficiency (SE) [8].

Maximum likelihood signal detection (MLD) [9] achieves a good BER performance without side-information (but note that the phase rotation patterns need to be shared by transmitter and receiver). MLD is done for all possible phase rotation patterns. The FD-SLM using MLD, called blind FD-SLM in this paper, was proposed for orthogonal frequency division multiplexing (OFDM) [10] and for SC-FDE [11]. Similar BER performance to ideal side-information sharing case is achieved. However, unlike the blind FD-SLM, simple binary phase rotation (i.e. ± 1) cannot be used in TD-SLM because of symmetric signal constellation. Therefore, an application of MLD in [11] to TD-SLM is not straightforward.

In this paper, we propose a blind polyphase TD-SLM for SC-FDE. Polyphase rotation patterns are used so that any unselected phase rotation pattern produces different signal constellation after multiplying its complex-conjugated version to the received signal. On the other hand, multiplying the complex-conjugated version of correct phase rotation pattern (i.e. selected pattern) to the received signal can perfectly remove the phase rotation due to TD-SLM and provides exactly the same constellation as the original signal constellation. Because of this nature, blind detection without side information is possible. The design criterion of polyphase rotation patterns for obtaining the above property is also introduced in this paper. In addition, the studies in [10-11] did not consider channel coding. The blind TD-SLM is also studied for turbo-coded SC-FDE in this paper.

The rest of this paper is organized as follows. Sect. II describes the idea of TD-SLM. Sect. III and IV present the transmitter using TD-SLM and the receiver without side information, respectively. Sect. V shows the computer simulation results, and Sect. VI concludes the paper.

II. Blind TD-SLM Algorithm

Assuming that an N_c-length time-domain transmit block is represented by a vector $\mathbf{s} = [s(0), s(1), \ldots, s(N_c-1)]^T$, PAPR of $\mathbf{s}$ calculated over an oversampled transmission block is expressed by

$$\mathrm{PAPR}(\mathbf{s}) = \frac{\max\{|s(n)|^2, n = 0, \frac{1}{V}, \frac{2}{V}, \ldots, N_c - 1\}}{\frac{1}{N_c}\sum_{n=0}^{N_c-1}|s(n)|^2}, \quad (1)$$

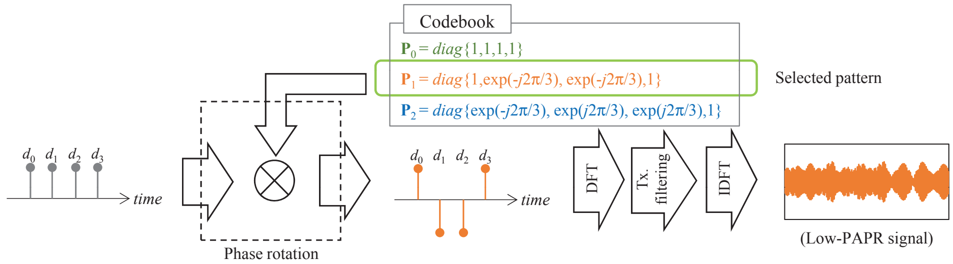

Fig. 1. Signal processing in TD-SLM.

where V is oversampling factor. TD-SLM algorithm considered in this paper is similar to the algorithm in [7], where its signal processing is illustrated by Fig. 1.

A codebook consisting of U different phase rotation patterns $\mathbf{P}_u = diag[P_u(0), \ldots, P_u(N_c-1)]$, $u = 0 \sim U-1$ is defined. In [7], the phase rotation patterns are set to be binary phase rotation, i.e. $P_u(n) = \pm 1$, $n = 0 \sim N_c - 1$, except the first pattern is set to be an identity matrix $\mathbf{I}_{N_c}$. However, the use of binary phase rotation causes false detection in transmission using TD-SLM when the blind phase rotation pattern estimation is applied at the receiver. In this paper, we alternatively use the polyphase rotations which are randomly generated as $P_u(n) \in \{e^{j0}, e^{j2\pi/3}, e^{j4\pi/3}\}$, $n = 0 \sim N_c - 1$, $u = 1 \sim U-1$. Note that the above polyphase rotation patterns are not optimal but sufficient for allowing the blind phase rotation pattern estimation. The details about phase rotation pattern design are further discussed in Sect. IV.

$\mathbf{P}_u$ is multiplied to data-modulated transmit block $\mathbf{d} = [d(0), \ldots, d(N_c-1)]^T$ for generating a candidate block $\mathbf{d}_u = \mathbf{P}_u\mathbf{d}$. All candidate blocks $\mathbf{d}_u$ are then passed through transmit signal processing (the details are described in Sect. III). The instantaneous PAPR of the u-th transmit waveform candidates $\mathbf{s}_u = [s_u(0), \ldots, s_u(N_c-1)]T$ is calculated by referring (1). The selected phase rotation pattern $\mathbf{P}_{\hat{u}}$, with the corresponding pattern index $\hat{u}$, is selected by the following criterion.

$$\mathbf{P}_{\hat{u}} = \arg \min_{u=0,1,\ldots,U-1} \text{PAPR}(\mathbf{s}_u = \mathbf{F}_{N_c}^H \mathbf{H}_T \mathbf{F}_{N_c} \mathbf{P}_u \mathbf{d}). \quad (2)$$

The definition of the remaining vectors and matrices representation is described in more details in Sect. III.

III. SC-FDE Transmitter with Polyphase TD-SLM

Single-user N_c-length block transmission with N_g-length of cyclic prefix (CP) insertion is assumed. Transmitter model of filtered SC-FDE equipped with TD-SLM is illustrated by Fig. 2(a). The binary information sequence is firstly encoded by turbo encoding, then the encoded binary sequence is data-modulated and divided into a transmit block consisting of N_c data-modulated symbols $\mathbf{d} = [d(0), \ldots, d(N_c-1)]^T$. The block $\mathbf{d}$ is used for generating U transmit block candidates for TD-SLM $\mathbf{d}_u$ by applying different phase rotation patterns. The u-th transmit block candidate is expressed by

$$\mathbf{d}_u = \mathbf{P}_u \mathbf{d}, \quad (3)$$

where $\mathbf{P}_u$ represents phase rotation matrix and the generation of $P_u(n)$ is already discussed in Sect. II. Each transmit

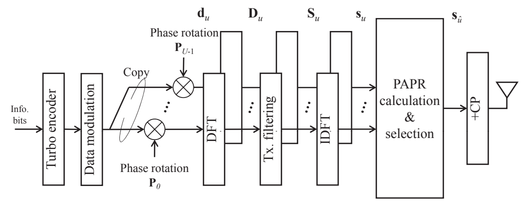

(a) Transmitter

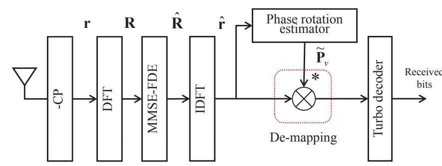

(b) Receiver

Fig. 2. Transceiver system models of SC-FDE using blind TD-SLM.

block candidate is transformed into frequency domain, yielding frequency-domain transmit signal of the u-th candidate $\mathbf{D}_u = [D_u(0), \ldots, D_u(N_c-1)]^T$ as

$$\mathbf{D}_u = \mathbf{F}_{N_c} \mathbf{P}_u \mathbf{d}, \quad (4)$$

where the N_c-point DFT matrix $\mathbf{F}_{N_c}$ is expressed by

$$\mathbf{F}_{N_c} = \frac{1}{\sqrt{N_c}} \begin{bmatrix} 1 & 1 & \cdots & 1 \\ 1 & e^{\frac{-j2\pi(1)(1)}{N_c}} & \cdots & e^{\frac{-j2\pi(1)(N_c-1)}{N_c}} \\ \vdots & \vdots & \ddots & \vdots \\ 1 & e^{\frac{-j2\pi(N_c-1)(1)}{N_c}} & \cdots & e^{\frac{-j2\pi(N_c-1)(N_c-1)}{N_c}} \end{bmatrix}, \quad (5)$$

and its Hermitian transpose $\mathbf{F}_{N_c}^H$ represents IDFT operation.

Next, $\mathbf{D}_u$ is multiplied by the transmit filtering matrix $\mathbf{H}_T = diag[H_T(0), \ldots, H_T(N_c-1)]$, yielding frequency-domain filtered signal $\mathbf{S}_u = \mathbf{H}_T \mathbf{D}_u$. Note that we apply the transmit filtering in frequency domain instead of in time domain since it can be applied as one-tap multiplication. Square-root raised cosine (SRRC) filter with roll-off factor α=0 is assumed in this paper. After that, $\mathbf{S}_u$ is transformed back into time domain by N_c-point IDFT matrix $\mathbf{F}_{N_c}^H$. PAPR calculation is applied in order to search and select the transmit signal with the lowest PAPR based on (2). The selected transmit signal based on TD-SLM is expressed by

$$\mathbf{s}_{\hat{u}} = \mathbf{F}_{N_c}^H \mathbf{H}_T \mathbf{F}_{N_c} \mathbf{d}_{\hat{u}} = \mathbf{F}_{N_c}^H \mathbf{H}_T \mathbf{F}_{N_c} \mathbf{P}_{\hat{u}} \mathbf{d}. \quad (6)$$

Finally, the last N_g samples of transmit block are copied as CP and inserted into the guard interval (GI), then a CP-inserted signal block of $N_g + N_c$ samples is transmitted.

IV. Receiver with Phase Rotation Estimation

A. Received Signal Representation

Receiver block diagram is illustrated by Fig. 2(b). The propagation channel is assumed to be a symbol-space L-path frequency-selective block Rayleigh fading channel [2], where its impulse response between transmitter and receiver is

$$h(\tau) = \sum_{l=0}^{L-1} h_l \delta(\tau - \tau_l), \tag{7}$$

where h_l and τ_l are complex-valued path gain and time delay of the l-th path, respectively. Time-domain received signal vector after CP removal $\mathbf{r} = [r(0), \ldots, r(N_c-1)]^T$ is expressed by

$$\mathbf{r} = \sqrt{2E_s/T_s}\mathbf{h}\mathbf{s}_{\hat{u}} + \mathbf{n}, \tag{8}$$

where $\mathbf{s}_{\hat{u}} = \mathbf{F}_{N_c}^H \mathbf{H}_T \mathbf{F}_{N_c} \mathbf{P}_{\hat{u}} \mathbf{d}$ is obtained from (6). E_s is symbol energy, and $\mathbf{n}$ is noise vector in which each element is zero-mean additive white Gaussian noise (AWGN) having the variance $\frac{2N_0}{T_s}$ with T_s is symbol duration and N_0 being the one-sided noise power spectrum density. Channel response matrix $\mathbf{h}$ is a circulant matrix representing time-domain channel response, which is

$$\mathbf{h} = \begin{bmatrix} h_0 & & & h_{L-1} & \cdots & h_1 \\ h_1 & \ddots & & & \ddots & \vdots \\ \vdots & & h_0 & \mathbf{0} & & h_{L-1} \\ h_{L-1} & & h_1 & \ddots & & \\ & \ddots & \vdots & & \ddots & \\ \mathbf{0} & & h_{L-1} & \cdots & \cdots & h_0 \end{bmatrix}. \tag{9}$$

The received signal vector $\mathbf{r}$ is transformed into frequency domain by N_c-point DFT, obtaining the frequency-domain signal $\mathbf{R}$ as

$$\begin{aligned} \mathbf{R} &= \sqrt{\tfrac{2E_s}{T_s}}\mathbf{F}_{N_c}\mathbf{h}\mathbf{F}_{N_c}^H \mathbf{H}_T \mathbf{F}_{N_c} \mathbf{P}_{\hat{u}} \mathbf{d} + \mathbf{F}_{N_c}\mathbf{n} \\ &= \sqrt{\tfrac{2E_s}{T_s}}\mathbf{H}_c \mathbf{H}_T \mathbf{F}_{N_c} \mathbf{P}_{\hat{u}} \mathbf{D} + \mathbf{N} \end{aligned}, \tag{10}$$

where the frequency-domain channel response $\mathbf{H}_c$ is defined by $\mathbf{H}_c \equiv diag[H_c(0), \ldots, H_c(N_c-1)] = \mathbf{F}_{N_c}\mathbf{h}\mathbf{F}_{N_c}^H$.

FDE based on minimum mean-square error criterion (MMSE-FDE) [1] is applied by multiplying the FDE matrix $\mathbf{W}_R = diag[W_R(0), \ldots, W_R(N_c-1)]$ to $\mathbf{R}$, yielding the received signal after equalization $\hat{\mathbf{R}} = \mathbf{W}_R\mathbf{R}$. The FDE weight at subcarrier k, $W_R(k)$, is derived so as to minimize the MSE between frequency-domain transmit vector $\mathbf{S}_{\hat{u}}$ and $\hat{\mathbf{R}}$, and is expressed by

$$W_R(k) = \frac{H_c^*(k)H_T^*(k)}{|H_c(k)H_T(k)|^2 + (E_s/N_0)^{-1}}, \tag{11}$$

where $H_c(k)$ is the k-th element in the diagonal of $\mathbf{H}_c$, which corresponds to the frequency-domain channel gain at the k-th subcarrier. Note that $W_R(k)$ is not a function of the selected phase rotation pattern, which is different from [6] and [11].

The signal after FDE $\hat{\mathbf{R}}$ is then transformed into time domain by N_c-point IDFT, yielding time-domain signal before de-mapping $\hat{\mathbf{r}} = [\hat{r}(0), \ldots, \hat{r}(N_c-1)]^T$ as

$$\hat{\mathbf{r}} = \mathbf{F}_{N_c}^H \hat{\mathbf{R}} = \sqrt{\frac{2E_s}{T_s}}\mathbf{F}_{N_c}^H \tilde{\mathbf{H}}_c \mathbf{F}_{N_c} \mathbf{P}_{\hat{u}} \mathbf{d} + \mathbf{F}_{N_c}^H \mathbf{W}_R \mathbf{F}_{N_c} \mathbf{n}, \tag{12}$$

where $\tilde{\mathbf{H}}_c = \mathbf{W}_R \mathbf{H}_c \mathbf{H}_T$ is the frequency-domain equivalent channel gain. The time-domain equalized signal at time index n, $\hat{r}(n)$, can be expressed by

$$\begin{aligned} \hat{r}(n) =& \sqrt{\tfrac{2E_s}{T_s}}\left(\tfrac{1}{N_c}\sum_{k=0}^{N_c-1}\tilde{H}_c(k)\right)P_{\hat{u}}(n)d(n) \\ &+ \sqrt{\tfrac{2E_s}{T_s}}\left(\tfrac{1}{N_c}\sum_{k=0}^{N_c-1}\tilde{H}_c(k)\sum_{n'\neq n}^{N_c-1}P_{\hat{u}}(n')d(n')e^{j2\pi\frac{n-n'}{N_c}}\right) \\ &+ \tilde{n}(n) \end{aligned}, \tag{13}$$

where $\tilde{n}(n)$ is the n-th element in $\tilde{\mathbf{n}} = \mathbf{F}_{N_c}^H \mathbf{W}_R \mathbf{F}_{N_c}\mathbf{n}$. It is seen that the first term in (13) represents the desired signal, where the rest are residual ISI and noise, respectively.

In TD-SLM, the time-domain received vector $\hat{\mathbf{d}} = [\hat{d}(0), \ldots, \hat{d}(N_c-1)]^T$ before turbo decoding is obtained by multiplying the complex-conjugated version of selected phase rotation, i.e. de-mapping [7], as $\hat{\mathbf{d}} = \mathbf{P}_{\hat{u}}^H \hat{\mathbf{r}}$. However, side-information transmission is required to let the receiver know the information of $\mathbf{P}_{\hat{u}}$. A phase rotation pattern estimation without side-information is introduced in the following sub-section. Finally, an estimated phase rotation pattern estimation $\tilde{\mathbf{P}}_v$ is used for de-mapping, yielding the symbols vector before turbo decoding $\hat{\mathbf{d}}$ as

$$\hat{\mathbf{d}} = \tilde{\mathbf{P}}_v^H \hat{\mathbf{r}} = \tilde{\mathbf{P}}_v^H \mathbf{F}_{N_c}^H \hat{\mathbf{R}}. \tag{14}$$

B. Phase Rotation Pattern Estimation

In [11], the MLD was proposed by utilizing the fact that the received symbols vector obtained from correct de-mapping and that of incorrect de-mapping are different and noticeable, where the difference is seen by calculating the MSE of received vector and the original constellations, that is

$$\tilde{\mathbf{P}}_v = \arg\min_{\substack{\mathbf{P}_v, v=0\sim U-1, \\ \tilde{\mathbf{d}}\in\Psi_{\text{mod}}}} \|\mathbf{F}_{N_c}^H \mathbf{P}_v^H \hat{\mathbf{R}} - \tilde{\mathbf{d}}\|^2 \text{ (for FD-SLM)}, \tag{15}$$

where Ψ_{mod} is a set of signal constellations of a particular modulation level. It is seen from the MLD in (15) that the de-mapping and MSE calculation is in different domains. In general, the hard-decision symbols vector $\tilde{\mathbf{d}}$ is obtained from (15) simultaneously, but it is not suitable for turbo-coded transmission since the decoder requires soft-decision value.

We alternatively introduce a new phase rotation pattern estimation for TD-SLM. Since the de-mapping and MSE calculation are carried out in the same domain in blind TD-SLM, the phase rotation pattern estimation for TD-SLM can be designed by considering (12), (14) and modifying (15) as

$$\tilde{\mathbf{P}}_v = \arg\min_{\substack{\mathbf{P}_v, v=0\sim U-1, \\ \tilde{\mathbf{d}}\in\Psi_{\text{mod}}}} \|\mathbf{P}_v^H \mathbf{F}_{N_c}^H \hat{\mathbf{R}} - \tilde{\mathbf{d}}\|^2. \tag{16}$$

It is observed that (16) is different from (15) since $\mathbf{P}_v^H$ is applied to time-domain vector $\hat{\mathbf{r}} = \mathbf{F}_{N_c}^H \hat{\mathbf{R}}$. Moreover, (16) requires less number of IDFT operations compared to (15) since $\hat{\mathbf{r}} = \mathbf{F}_{N_c}^H \hat{\mathbf{R}}$ is identical for all computation times $v = 0 \sim U-1$. The hard-decision symbols vector can be obtained simultaneously if there is no channel coding. With the aid of shared codebook, the phase rotation pattern estimation in (16) can reduce the number of complex-valued multiplication from $3^{N_c} \times N_c \times N_{\text{mod}}^2$ to $U \times N_c \times (N_{\text{mod}}^2 + 1)$, where N_{mod} represents modulation level (2 for 4QAM, 4 for 16QAM and 6 for 64QAM).

Meanwhile, the phase rotation pattern estimation without side-information in (16) can be effectively used if the following criteria are met [10-11]:

- The set of phase rotation patterns $\{\mathbf{P}_u, u = 0 \sim U-1\}$ is fixed for every transmit block and is known *apriori*.
- $c(n)P_u(n) \notin \Psi_{\text{mod}}$ for all $n = 0 \sim N_c-1$, $u = 0 \sim U-1$ and for a given $\mathbf{c} = [c(0), \ldots, c(N_c-1)]^T$ and $\mathbf{c} \in \Psi_{\text{mod}}$. In other words, the phase-rotated symbols vector needs to be sufficiently different from the original constellations. This criterion leads to the difference between received vector with correct de-mapping and incorrect de-mapping.

The first criterion is cleared by using a shared codebook. However, the second criterion cannot be accomplished if the binary phase rotation pattern (± 1) is used in the TD-SLM. The above fact leads to the necessity of developing the phase rotation patterns for allowing the blind TD-SLM.

It is known from [12] that the phase rotation patterns should be randomly generated and uniformly distributed in [0, 2π) in order to achieve the lowest PAPR in SLM. However, phase rotation distribution with the interval of $2\pi/A$ when A is even (e.g. $P_u(n) \in \{e^{j0}, e^{j(2\pi/4)}, e^{j(4\pi/4)}, e^{j(6\pi/4)}\}$ when A=4) cannot be used since the criterion of $c(n)P_u(n) \notin \Psi_{\text{mod}}$ is violated. On the other hand, $c(n)P_u(n) \notin \Psi_{\text{mod}}$ is accomplished when A is odd number, and hence the discrete, uniformly-distributed phase rotation $P_u(n) \in \{e^{j0}, e^{j(2\pi/3)}, e^{j(4\pi/3)}\}$ (i.e. A=3) is selected to be used in the TD-SLM in this paper. Note that the decision of using $P_u(n) \in \{e^{j0}, e^{j(2\pi/3)}, e^{j(4\pi/3)}\}$ is not defined as an optimal pattern but sufficient for allowing blind TD-SLM.

In addition, Fig. 3 shows one-shot observation of $\tilde{\mathbf{P}}_v^H \hat{\mathbf{r}}$ in SC-FDE using blind TD-SLM with 16QAM modulation at average received bit energy-to-noise power spectrum density ratio E_b/N_0=20 dB, where $E_b/N_0 = (1/N_{\text{mod}})(E_s/N_0)(N_c/(N_c+N_g))$. It is seen that $\tilde{\mathbf{P}}_v^H \hat{\mathbf{r}}$ is very close to the original 16QAM signal constellations if the estimation is correct as $\tilde{\mathbf{P}}_v = \mathbf{P}_{\hat{u}}$, while most symbols in $\tilde{\mathbf{P}}_v^H \hat{\mathbf{r}}$ are apart from the original constellations when $\tilde{\mathbf{P}}_v \neq \mathbf{P}_{\hat{u}}$. This also confirms that the phase rotation pattern estimation in (16) has a potential to achieve high accuracy when the received power is sufficiently high.

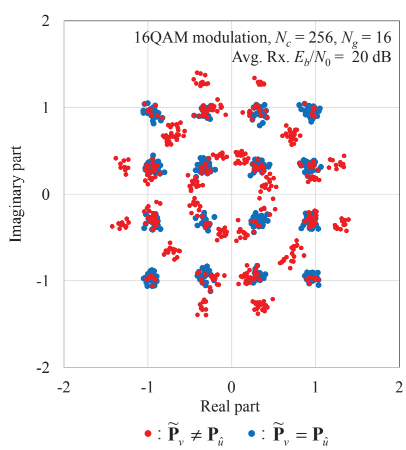

Fig. 3. One-shot observation of received symbols after de-mapping.

TABLE I
SIMULATION PARAMETERS.

Transmitter	Modulation	4QAM, 16QAM, 64QAM
	FFT/IFFT block size	N_c=256
	Cyclic prefix length	N_g=16
	Transmit filtering	SRRC (α=0)
	SLM type	Blind TD-SLM
	Phase rotation sequence type	Random polyphase $\{e^{j0}, e^{j(2\pi/3)}, e^{j(4\pi/3)}\}$
Turbo coding	Encoder	(13, 15) RSC encoders
	Decoder	Log-MAP w/ 6 iterations
	Coding rate	R=3/4
Channel	Fading type	Frequency-selective block Rayleigh
	Power delay profile	16-path uniform
Receiver	Channel estimation	Ideal
	FDE	MMSE-FDE

V. PERFORMANCE EVALUATION

Numerical and simulation parameters are summarized in Table 1. Oversampling factor is set to be V=8. System performances are evaluated in terms of PAPR and BER.

A. PAPR Performance

PAPR performance is evaluated by measuring the PAPR value at complementary cumulative distribution function (CCDF) equals 10^{-3}, called $\text{PAPR}_{0.1\%}$, where its definition is expressed by $prob(\text{PAPR}(\mathbf{s}) \geq \text{PAPR}_{0.1\%}) = 10^{-3}$.

Fig 4(a) shows the $\text{PAPR}_{0.1\%}$ of SC-FDE using the blind TD-SLM and the blind FD-SLM as a function of number of phase rotation patterns (U). The performance of SC-FDE using FD-SLM is evaluated by referring [11]. The $\text{PAPR}_{0.1\%}$ of conventional SC-FDE is shown at the place with U=1. It is seen that $\text{PAPR}_{0.1\%}$ decreases when U increases in both SLM approaches because of higher probability to obtain the transmit waveform with lower PAPR among the candidates. SC-FDE using blind TD-SLM also achieves lower $\text{PAPR}_{0.1\%}$ compared to FD-SLM in every U. In particular, up to 3.2 dB of PAPR reduction is achieved when U=512 and assuming 64QAM data modulation in SC-FDE using blind TD-SLM, while the maximum of PAPR reduction in FD-SLM is 2 dB. The reason is already discussed in [7] as the resultant signal amplitude in SC-FDE using blind TD-SLM is in a bound set while that of FD-SLM is very close to Gaussian distribution, resulting in the TD-SLM has higher probability to achieve the near-optimal transmit waveform. In addition, $\text{PAPR}_{0.1\%}$ of the blind TD-SLM in Fig. 4(a) is same as in [7] even though the polyphase rotations are applied instead of binary phase rotation.

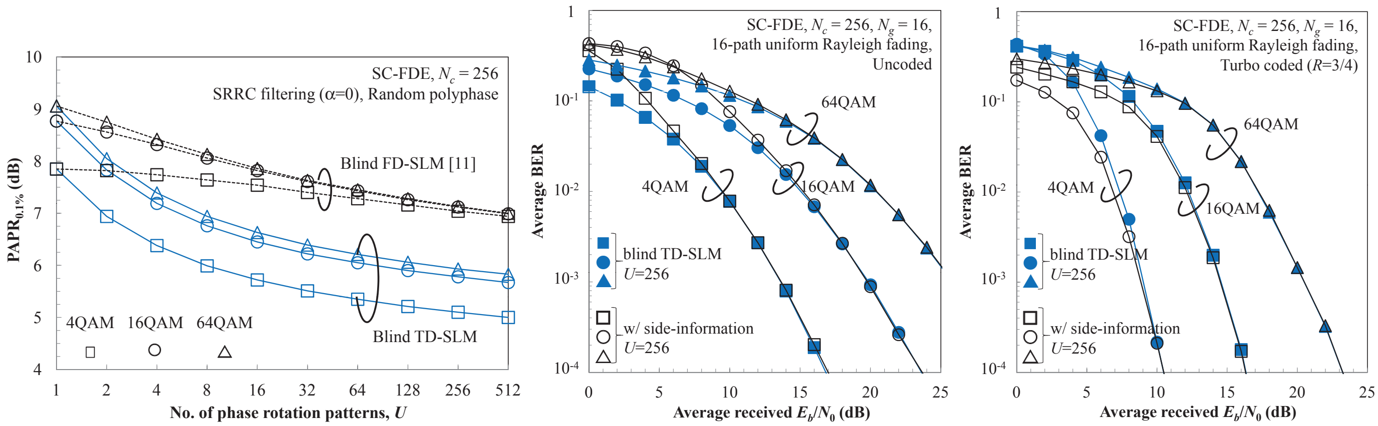

(a) PAPR versus number of phase rotation patterns (b) BER (Uncoded) (c) BER (Turbo-coded with R=3/4)

Fig. 4. Performance evaluation.

B. BER Performance

Fig. 4(b) and Fig. 4(c) show the BER as a function of average received E_b/N_0 of SC-FDE using blind TD-SLM assuming uncoded transmission and turbo-coded transmission with coding rate R=3/4, respectively. The number of phase rotation patterns U is set to be 256. BER performance of TD-SLM with ideal side-information detection is also shown for comparison. It can be seen that BER performances of SC-FDE using blind TD-SLM degrade at a low received E_b/N_0 region. The above result can be described by referring (13) and (16) as the effect from noise and residual ISI causes difficulty in phase rotation pattern estimation. The residual ISI and noise power make $\tilde{\mathbf{P}}_v^H \hat{\mathbf{r}}$ become apart from original constellations even though the de-mapping is organized correctly, i.e. $\tilde{\mathbf{P}}_v = \mathbf{P}_{\hat{u}}$.

However, the BER performance of SC-FDE using blind TD-SLM becomes similar to that of SC-FDE using TD-SLM with ideal side-information detection when $E_b/N_0 \geq 8$ dB for 4QAM and 64QAM, and $E_b/N_0 \geq 12$ dB for 16QAM in case of uncoded transmission. The similar results are also achieved in case of turbo-coded transmission with R=3/4. The above results conclude that the proposed SC-FDE with blind TD-SLM using polyphase rotation can be used effectively when E_b/N_0 is sufficiently high without requirement of side-information transmission, and hence the SE degradation due to side-infotmation sharing can be prevented.

VI. Conclusion

Blind TD-SLM with polyphase rotations for filtered SC-FDE was proposed. The signal detection is carried out by calculating the MSE of the received block candidates generated from a set of phase rotation patterns and the original constellations. We also introduced the design criteria for polyphase rotations in order to allow the blind TD-SLM. Simulation results confirmed that the proposed blind TD-SLM achieves low-PAPR transmission without degradation in BER while transmitting no side-information.

In addition, blind TD-SLM requires high computational complexity due to candidate generation at the transmitter and MLD at the receiver, and hence, a study on complexity-reduced blind SLM remains as our important future work.

Acknowledgment

This paper includes a part of results of "The research and development project for realization of the fifth-generation mobile communications system" (#0155-0019, April 2016) commissioned to Tohoku University by The Ministry of Internal Affairs and Communications (MIC), Japan.

References

[1] D. Falconer et al., "Frequency domain equalization for single-carrier broadband wireless systems," *IEEE Commun. Mag.*, Vol. 40, No. 4, pp. 58-66. Apr. 2002.

[2] A. Goldsmith, *Wireless Communications*, Cambridge Press, 2005.

[3] S. Okuyama et al., "MMSE Frequency-domain Equalization Using Spectrum Combining for Nyquist Filtered Broadband Single-Carrier Transmission," *in Proc. IEEE Veh. Technol. Conference (VTC 2010-Spring)*, Taipei, Taiwan, May 2010.

[4] J. Joung et al., "A Survey on Power-Amplifier-Centric Techniques for Spectrum- and Energy-Efficient Wireless Communications," *IEEE Commun. Survey & Tutorial*, Vol. 17, No. 1, pp. 315-333, 1Q 2015.

[5] R. W. Bauml et al., "Reducing the Peak-to-Average Power Ratio of Multicarrier Modulation by Selected Mapping," *IEEE Electron. Lett.*, Vol. 32, No. 22, pp. 2056-2057, Oct. 1996.

[6] A. Boonkajay et al., "Selective Mapping for Broadband Single-Carrier Transmission Using Joint Tx/Rx MMSE-FDE," *in Proc. IEEE Int. Symp. on Personal Indoor and Mobile Radio Commun. (PIMRC 2013)*, London, U.K., Sept. 2013.

[7] A. Boonkajay and F. Adachi, "Low-PAPR Joint Transmit/Received SC-FDE Transmission using Time-Domain Selected Mapping," *in Proc. Asia-Pacific Conference on Commun. (APCC 2014)*, Pattaya, Thailand, Oct. 2014.

[8] S. S. Eom et al., "Low-Complexity PAPR Reduction Scheme Without Side Information for OFDM Systems," *IEEE Trans. Signal Process.*, Vol. 60, No. 7, pp. 3657-3669, Jul. 2012.

[9] J. G. Proakis and M. Salehi, *Digital Communications*, 5^{th}ed., McGraw-Hill, 2008.

[10] A. D. S. Jayalath and C. Tellambura, "SLM and PTS peak-power reduction of OFDM signals without side information," *IEEE Trans. Wireless Commun.*, Vol. 4, No. 5, pp. 2006-2013, Sept. 2005.

[11] A. Boonkajay and F. Adachi, "A Blind Selected Mapping Technique for Low-PAPR Single-Carrier Signal Transmission," *in Proc. Int. Conference on Inform. Commun. and Signal Process. (ICICS 2015)*, Singapore, Dec. 2015.

[12] G. T. Zhou and L. Peng, "Optimality Condition for Selected Mapping in OFDM," *IEEE Trans. Signal Process.*, Vol. 54, No. 8, pp. 3159-3165, Aug. 2006.